Negative differential resistance and threshold-switching in conical nanopores with KF solutions ᴱᴾ

Patricio Ramirez, Jose J. Perez-Grau, Javier Cervera, Saima Nasir, Mubarak Ali, Wolfgang Ensinger, and Salvador Mafe

COLLECTIONS

EP   This paper was selected as an Editor's Pick

View Online   Export Citation   CrossMark

Negative differential resistance and threshold-switching in conical nanopores with KF solutions (EP)

Patricio Ramirez,[1,a)] (iD) Jose J. Perez-Grau,[1] Javier Cervera,[2] (iD) Saima Nasir,[3,4] (iD) Mubarak Ali,[3,4] (iD) Wolfgang Ensinger,[3,5] and Salvador Mafe[2] (iD)

AFFILIATIONS

[1]Departament de Física Aplicada, University Politècnica de València, E-46022 Valencia, Spain
[2]Departament de Física de la Terra i Termodinàmica, Universitat de València, E-46100 Burjassot, Spain
[3]Department of Material- and Geo-Sciences, Materials Analysis, Technische Universität Darmstadt, Alarich-Weiss-Str. 02, D-64287 Darmstadt, Germany
[4]Materials Research Department, GSI Helmholtzzentrum für Schwerionenforschung, Planckstrasse 1, D-64291 Darmstadt, Germany
[5]Center for Synthetic Biology, TU Darmstadt, 64283 Darmstadt, Germany

a)Author to whom correspondence should be addressed: patraho@fis.upv.es

ABSTRACT

Negative differential resistance (NDR) phenomena are under-explored in nanostructures operating in the liquid state. We characterize experimentally the NDR and threshold switching phenomena observed when conical nanopores are immersed in two identical KF solutions at low concentration. Sharp current drops in the nA range are obtained for applied voltages exceeding thresholds close to 1 V and a wide frequency window, which suggests that the threshold switching can be used to amplify small electrical perturbations because a small change in voltage typically results in a large change in current. While we have not given a detailed physical mechanism here, a phenomenological model is also included.

Published under license by AIP Publishing. https://doi.org/10.1063/5.0051422

Negative differential resistance (NDR) and threshold switching phenomena occur when the electrical current decreases sharply as the applied voltage is increased beyond a threshold value. These phenomena have been mostly reported in solid state components where they can find application in fast switches, memories, and logic devices. However, they are under-explored in nanostructures operating in the liquid state. Here, we characterize experimentally and theoretically the NDR and threshold switching phenomena observed when polymeric conical nanopores are immersed in between two identical KF solutions at low concentration. Sharp current drops in the nA range are obtained in the current (I)–voltage (V) curves when the applied voltages exceed thresholds of the order of 1 V over a wide frequency range. This fact suggests that the threshold switching can amplify small electrical perturbations because a small change in voltage typically results in a large change in current, a potentially useful characteristic for nanofluidic applications.[1–3] While we have not provided a detailed physical mechanism at this preliminary stage, a phenomenological model is also included.

Previous work in the field concerns different phenomena, including the negative incremental resistance and calcium-induced gating observed in asymmetric nanopores,[4] the NDR resulting from the external imposition of a mechanically forced electroosmotic flow through nanopores,[5] the electrical field regulation of ion transport in polyethylene terephthalate nanochannels,[6] SiN_x nanostructures,[7] and ionic-liquid/water mixtures,[8] and the electrodiffusion osmosis-induced NDR in pH-regulated mesopores.[9] Here, we focus on the characterization of ionic conduction in negatively charged single conical nanopores under different experimental conditions, showing that the NDR and threshold switching could be used to amplify small electrical perturbations because a small change in voltage typically results in a large change in current. Memory and memristor-like characteristics are also implied because the redistribution of ions and water molecules at the pore tip following the external time-dependent perturbations is not instantaneous. We believe that as NDR nanodevices extend further, new concepts and applications will find their way.

Figure 1 shows the setup used to conduct the I–V measurements. The single-pore PI membranes are obtained by irradiating the foils with heavy ions and the subsequent asymmetric chemical etching of the resulting ion tracks using a strong inorganic etchant (NaOCl) at
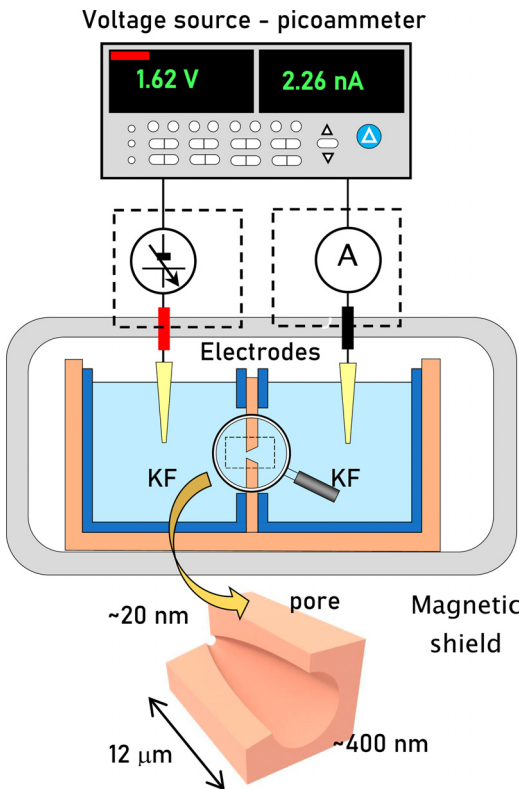
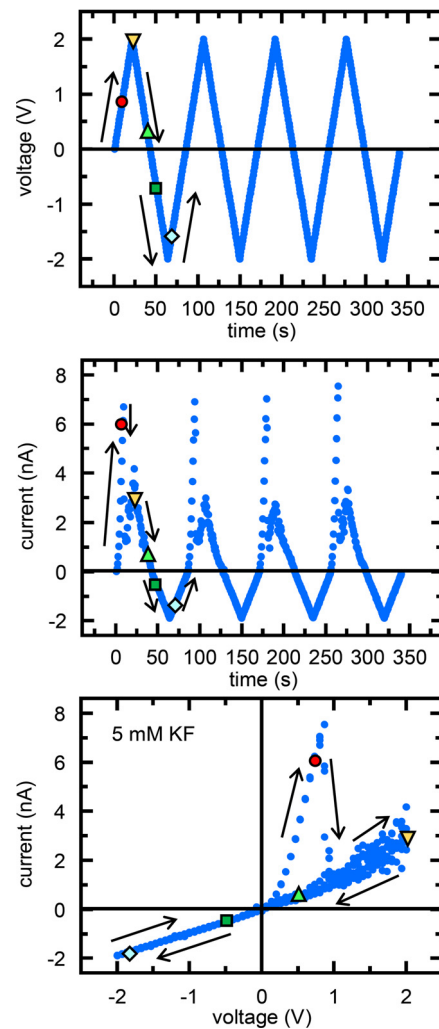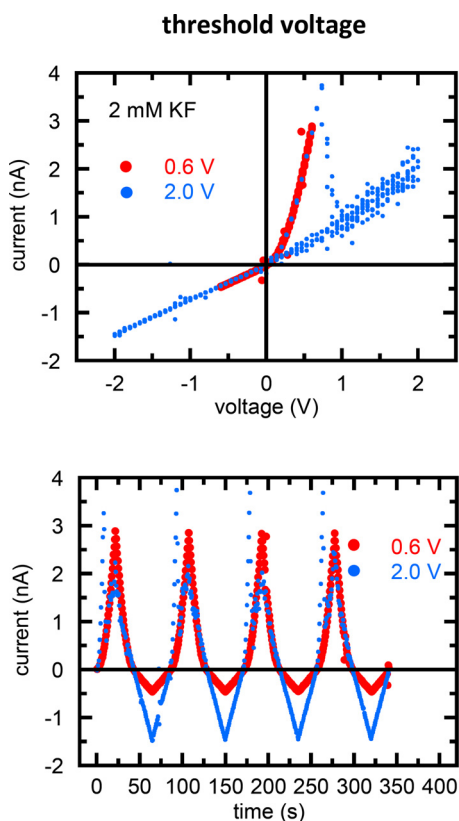**FIG. 1.** Scheme of the experimental setup. The ground electrode is placed on the pore base side.

FIG. 2. V–t (top) and I–t (center) temporal traces and I–V curves (bottom) obtained with sample 1, and the KF concentration is shown in the inset. From pore conductance measurements at high KCl concentrations, the estimated pore tip and base radii are 10 nm and 300 nm, respectively.

high temperature. The single-pore polyimide (PI) membrane is immersed in between two identical salt solutions at the concentration c and no buffer solution is added. The measured pH values are between 6.5–7.0, which are higher than the typical pK_a values of the surface pore COOH groups.[10,11] At this pH, the carboxylic acid groups $-COOH$ functionalized on the pore surface are in the ionized form $-COO^-$, which results in a negative fixed charge density.[10,11] The approximately conical pore geometry is characterized by the radii, which can be obtained from the pore imaging (base radius) and electrical conductance measurements (tip radius).[10–13] The pore radii are in the ranges 100–400 nm for the cone base and 10–40 nm for the cone tip.[14,15]

The electrical measurements are conducted using a voltage-source picoammeter (Keithley Instruments, Cleveland, Ohio) and Ag|AgCl electrodes with 2M KCl solution salt bridges. In some of the control experiments, Pt electrodes and Ag|AgCl electrodes without salt bridges are employed. The electrochemical cell is placed within a double-layered magnetic shield (Amuneal Manufacturing, Philadelphia, PA) to avoid environmental electrical perturbations. Before each measurement, the single-pore membrane is allowed to equilibrate with the aqueous salt (KF, KCl, KBr, KI) solution of concentration in the range 1–100 mM.

Figure 2 shows the V-time (t) and I–t traces together with the I–V curves obtained at $c = 5$ mM KF. A NDR region with a peak-to-valley current ratio close to 10 is clearly observed for voltages $V > 0$.

The arrows shown in Fig. 2 describe the time evolution of the current following the applied potential. The colored symbols approximately show particular voltage and current pairs through the imposed electrical cycle. This behavior is reminiscent of a threshold-switching memristor at $V > 0$ when a threshold voltage V_T is exceeded.[16]

To characterize further the above switching between the two conductance levels of Fig. 2, the different I–V curves and I–t traces are measured below ($V = 0.6$ V) and above ($V = 2$ V) the threshold value $V_T = 0.8$, as shown in Fig. 3. As it could be expected, the NDR region and the threshold voltage depend on the KF salt solution concentration that modulates the availability of the electrical carriers (ions) in the pore, as shown in Fig. 4. Note that because of the negative surface charge, the F^- ions (*coions*) tend to be excluded from the pore
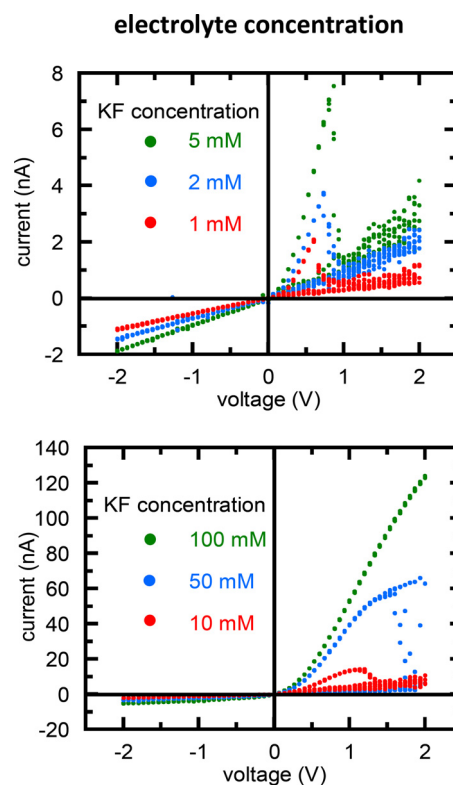
threshold voltage

electrolyte concentration

FIG. 4. $I-V$ curves obtained with sample 1, and the KF concentrations shown in the insets for sample 1.

FIG. 3. $I-V$ curves (top) and $I-t$ traces (bottom) obtained with sample 1, and the KF concentration shown in the inset for voltages below (0.6 V) and above (2 V) the threshold voltage of Fig. 2.

solution, while the K^+ ions (*counterions*) enter the pore to keep local electroneutrality.[11]

Figure 4 concerns a wide concentration range, $c = 1-100$ mM. Remarkably, the threshold voltage increases with the KF concentration and is not observed at high enough concentrations above 100 mM KF, even at voltages as high as 4 V (not shown in Fig. 4).

In order to check further the reproducibility of the phenomena observed and understand the underlying physico-chemical mechanisms, we conducted four additional control experiments (Figs. S1−S5 of supplementary material). Figure S1 together with previous experiments conducted at higher concentrations[17] shows that other halide ions (Cl^-, Br^-, and I^-) and potassium salts (KCl, KBr, and KI) do not show the NDR and threshold phenomena of Fig. 2, which points out the central role of F^-. On the contrary, experiments conducted with LiF and NaF (not shown here) also displayed the observed threshold voltage behavior, thus discarding specific effects due to the counterion-dominated pore swelling at low salt concentrations—note the significantly different hydration energies of cations Li^+ and K^+. Note also the fact that the anion pore entrance that occurs at $V > 0$ [see Figs. 3(c) and 3(f) of Ref. 11] increases the pore conductance for all coions except for F^- at the threshold switching (Fig. S1).

Figure S2 emphasizes the role of the pore charges: the phenomena reported here are only observed in nanopores with relatively small pore openings, which corresponds to high fixed charge concentrations

at the pore tip region that modulates ionic selectivity and conduction.[11] Thus, we anticipate that different nanostructures with multiple NDR regions could be experimentally realized. In particular, cylindrical and cigar-shaped pores[18] with small enough radii may show NDR and threshold-switching phenomena at voltages $V > 0$ and $V < 0$. Figure S3 shows the effects associated with the position of the KF salt with respect to the pore tip. The NDR is observed at $V > 0$ only when it is the F^- ion rather than the Cl^- ion that enters the pore base and proceeds then to the tip where it encounters the kinetic barrier due to the high concentration of negative charges on the pore surface.[11] Interestingly, preliminary measurements conducted with PI pores functionalized with polyethyleneimine (PEI) chains do not show NDR phenomena (not shown here), as expected for a positively charged pore tip that does not constitute now a kinetic barrier for the F^- ion.

Figure S4 shows again the central role of the nanopore rather than the electrode type in the observed NDR and switching phenomena: the different electrodes (Pt electrodes and Ag|AgCl electrodes with and without salt bridges) employed do not affect the qualitative nature of the $I-V$ curves and $I-t$ traces obtained in the experiments.

To better characterize the signal type and frequency window where the threshold switching occurs, Fig. S5 shows the cases of white noise (*top*) and triangular scan rates of different frequencies (*bottom*) in the range 1–100 mHz. Clearly, a relatively fast white noise signal of frequency on the order of 1 Hz favors the high rather than the low

pore conductance state (Fig. S5, *top*), suggesting that the latter state is only achieved at low enough scan rates. Indeed, Fig. S5 (*bottom*) shows that the NDR occurs at low threshold voltages for a wide range of slow signals, while it tends to become less noticeable at high threshold voltages for high scan rates. These experimental facts are suggestive of kinetic limitations in the electrical conductance due to the redistribution of ions and solvent molecules at the nanoscale pore tip[11] that is forced by the time varying voltage, as shown by the KF solution position (Fig. S3) and signal frequency (Fig. S5) effects. However, using slow signals of the order of 0.1 Hz should not pose a serious problem in most sensing applications.

The remarkable switching and NDR phenomena observed here are reproducible and have been established in distinct pore samples under different conditions (Figs. 2–4) together with additional control experiments (Figs. S1–S5). Although the underlying ionic conduction processes occurring in the pore are not fully understood yet, we may tentatively offer some qualitative physical insights. The F^- ion has a low ionic radius compared with those of Cl^-, Br^-, and I^- anions, which suggest a high charge density because of its small size. Thus, fluoride ions show a high hydration energy, can have a second hydration shell, and tend to strongly immobilize the surrounding water molecules, especially in nanoscale environments.[19] In addition, hydrophobic interactions could be relevant and, in addition, a fraction of the fluoride ions in the pore solution may hydrolyze.[20] This is not the case of Cl^- and the corresponding strong acid HCl, and the fact is that the $I-V$ curves of the other halides (KCl, KBr, and KI) do not show the switching voltage and NDR characteristics of KF salts at low concentrations (Figs. 4 and S1). However, additional control experiments (not shown here) suggested a limited role of the pH for the limited range of values used here.

Recently, trigger voltage thresholds have also been reported in narrow pores and the possible role of the fixed charge groups mentioned.[7] The transient characteristics observed in the I–V curves have been ascribed to the particular chemistry of trivalent cations in PET nanochannels.[7] The effects of a voltage-triggered structural switching and swelling effects in polyelectrolyte-modified nanochannels have also previously been considered.[21] However, the previous characterization by electron microscopy of asymmetric nanopores in polyimide membranes[12] does not suggest dramatic structural changes in our case. The similarities between the transport of ionic-liquid/water mixtures in PET conical pores and typical memristor characteristics have been noted in 1-butyl-3-methylimidazolium tetrafluoroborate ([BMIM][BF4]) solutions, and the origin of the hysteresis loop was ascribed to the adsorption/desorption of the $[BMIM]^+$ cations on the pore surface.[8] However, all the above experimental contexts[4–9] are significantly different from that described above concerning the particular characteristics of the F^- ion.

A typical value[19] for the hydrated F^- radius is 0.35 nm, which is small compared with the pore tip radius (Fig. 1). Also, the typical solution Debye lengths are in the range $L_D = 1$ nm (solution concentration $c = 100$ mM) and 3 nm ($c = 10$ mM). These values suggest that hard-sphere steric effects only are not responsible for the observed behavior, but, on the contrary, the Debye screening of the pore charges should be significant here.[11,22] In particular, Figs. 3 and S3 show that the NDR is observed only when the F^- coion enters the pore base and proceeds then to the tip facing the electrode at voltage $V > V_T > 0$, where it encounters a kinetic barrier due to the high concentration of

negative charges fixed on the pore surface. Figures 4 and S5 suggest that this barrier can only be overcome at high salt concentrations, provoking a strong Debye screening of the pore tip charges[11] and at high signal frequencies avoiding the progressive accumulation of F^- ions at the pore tip barrier, respectively.

Note also that the electrical relaxation of the pore should be modulated by the free water networks available for ionic conduction at the pore tip together with the interaction between the hydrated $-COO^-$ groups at the pore surface and the neighboring solution counterions (K^+).[11] Conceivably, these characteristics should depend on the salt and pore properties and impose kinetic limitations to both the effective number of free electric carriers available for conduction and their mobility. Indeed, the high charge concentration at the pore tip is central to the observed phenomena, as shown by the control experiments of Figs. S2 and S3. According to this interpretation, threshold voltage and conductance kinetic limitations should be apparent neither for wide nanopore openings where the pore tip charge concentration is small (Fig. S2) nor for high salt concentrations giving low kinetic barriers because of the increased Debye screening of the pore fixed charges (Fig. 4), as observed experimentally. These arguments could explain the rather surprising result of observing a threshold voltage that increases rather than decreases with the electrical carrier concentration (Fig. 4).

The limited qualitative understanding of the observed phenomena, together with the fact that the pore tip could be in the limit between the continuum mean field description and the microscopic charge correlation theories,[22] makes it difficult the use of detailed models and suggests the consideration of a phenomenological approach where the pore solution transits between the low and high electrical resistance levels of Fig. 2 at the switching point. The two conductive pore states connected by the NDR region can then be reached following the voltage time cycle passing through the threshold V_T (Fig. 2). We tentatively introduce a threshold model of a memresistive device discussed by Pershin and Di Ventra,[16] where the nanopore resistance R_{on} of the high conductance (low resistance) regime changes with time following the V cycle (Fig. 2):

$$\frac{dR_{on}}{dt} = \left[\beta V + 0.5(\alpha - \beta)(|V + V_T| - |V - V_T|) \right]$$
$$\times H(R_{on} - R_{min})H(R_{max} - R_{on}). \quad (1)$$

In this model, α and β are constants that give the rate of change of R_{on} below and above V_T, respectively, and H is the Heavyside function that makes this rate to be non-zero only in the range $R_{min} < R_{on} < R_{max}$. Note that the nanopore resistance of the low conductance (high resistance) regime takes the constant value R_{off}. Figure 5 shows that the $I-V$ and $I-t$ theoretical curves obtained with this model can provide a qualitative description of the observed phenomena (Figs. 2 and 3). By introducing a concentration-dependent threshold voltage V_T in the above equation, other experimental results (Fig. 4) could also be rationalized.

We associate the switching of the nanopore resistance with the progressive accumulation and depletion of F^- ions occurring at $V > 0$ and $V < 0$, respectively.[11] At a certain value $V_T > 0$, enough fluoride ions strongly interact with the surrounding water molecules accumulated at the nanoscale barrier created by the negative pore tip charges. Accordingly, the aqueous channels needed for ionic conduction are decreased at the rate limiting pore tip. Also, this decreases in the free

Results of the memristive model
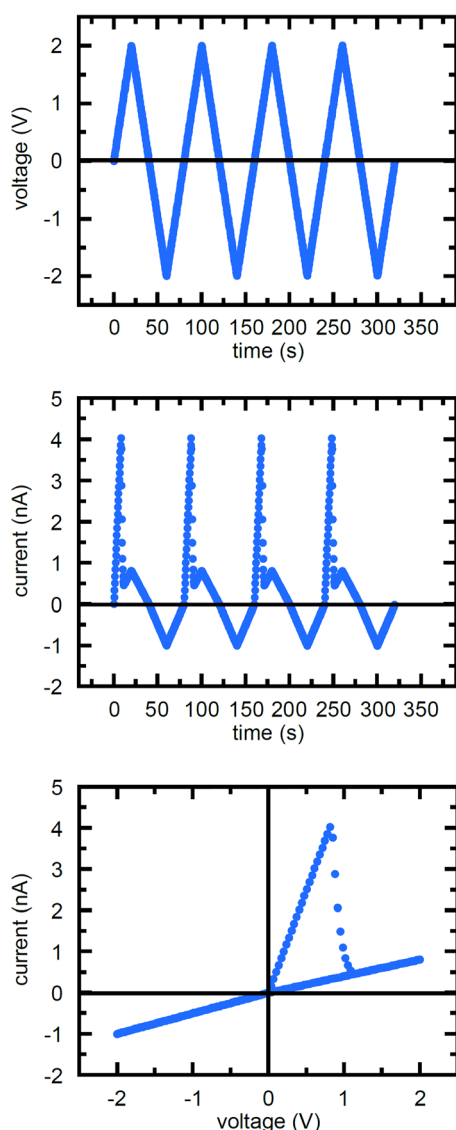
FIG. 5. Theoretical $I-V$ and $I-t$ curves obtained with the threshold model for the two-level pore conductance. We assume $\alpha = 0\,M\Omega\,V^{-1}\,s^{-1}$ and $\beta = 5\,M\Omega\,V^{-1}\,s^{-1}$ for the resistance rate and introduce the typical nanopore parameters $V_T = 0.8\,V$, $R_{min} = 0.2\,R_{max}$, with $R_{max} = 1\,M\Omega$ and $R_{off} = 2\,M\Omega$ at negative voltages. The initial value $R_{on} = 1.01\,R_{min}$ set at the beginning ($V=0$) of the first-time cycle should be reset at every new period for the pore to escape from the low conductance level R_{off} reached at $V < 0$, as observed experimentally (see the time cycle of Fig. 2). The reset value needs to be higher than R_{min} to avoid the pore being stuck in R_{min} following the temporal change of R given by the model.

water provoke that the counterions (K^+) interact more strongly with the $-COO^-$ groups at the pore surface. Conceivably, these processes should lead to a decreased electrical conductance at $V > V_T$. On the contrary, the strongly hydrated F^- ions are progressively depleted from the pore tip barrier for the rectified currents occurring at $V < 0$.

Thus, the pore can eventually recover the high conductance state at the beginning of next cycle to positive voltages starting at $V = 0$ (Fig. 5).

In conclusion, we have characterized experimentally and theoretically the NDR and threshold voltage switching phenomena occurring at the nanoscale in conical nanopores immersed in KF solutions at low concentration, emphasizing the role of the pore tip in the observed phenomena. The sharp current drop in the nA range obtained in the $I–V$ curves when the applied voltages exceed potential differences of the order of 1 V suggests that NDR and threshold switching phenomena could be used to amplify small electrical perturbations based on the redistribution of ions and water molecules at the pore tip. Memory and memristor-like characteristics could now be explored.[16] In particular, memristive devices based on ion channel-doped biomembranes can act as synaptic mimics,[23] and this could also be the case of biomimetic nanopores.

See the supplementary material for the results of the control experiments.

DATA AVAILABILITY

The data that support the findings of this study are available from the corresponding author upon reasonable request.

REFERENCES

[1]Z. Zhu, D. Wang, Y. Tian, and L. Jiang, J. Am. Chem. Soc. **141**, 8658 (2019).

[2]T. Ma, J.-M. Janot, and S. Balme, Small Methods **4**, 2000366 (2020).

[3]G. Pérez-Mitta, M. E. Toimil-Molares, C. Trautmann, W. A. Marmisollé, and O. Azzaroni, Adv. Mater. **31**, 1901483 (2019).

[4]Z. S. Siwy, M. R. Powell, E. Kalman, R. D. Astumian, and R. S. Eisenberg, Nano Lett. **6**, 473 (2006).

[5]L. Luo, D. A. Holden, W. J. Lan, and H. S. White, ACS Nano **6**, 6507 (2012).

[6]Y. Li, G. Du, G. Mao, J. Guo, J. Zhao, R. Wu, and W. Liu, ACS Appl. Mater. Interfaces **11**, 38055 (2019).

[7]I. W. Leong, M. Tsutsui, S. Murayama, T. Hayashida, Y. He, and M. Taniguchi, ACS Appl. Mater. Interfaces **12**, 52175 (2020).

[8]Q. Sheng, Y. Xie, J. Li, X. Wang, and J. Xue, Chem. Commun. **53**, 6125 (2017).

[9]C. Y. Lin, P. H. Wong, P. H. Wang, Z. S. Siwy, and L. H. Yeh, ACS Appl. Mater. Interfaces **12**, 3198 (2020).

[10]Z. Siwy, I. D. Kosinska, A. Fulinski, and C. R. Martin, Phys. Rev. Lett. **94**, 048102 (2005).

[11]J. Cervera, B. Schiedt, R. Neumann, S. Mafe, and P. Ramirez, J. Chem. Phys. **124**, 104706 (2006).

[12]Z. Siwy, D. Dobrev, R. Neumann, C. Trautmann, and K. Voss, Appl. Phys. A **76**, 781 (2003).

[13]P. Apel, Radiat. Meas. **34**, 559 (2001).

[14]P. Ramirez, V. Garcia-Morales, V. Gomez, M. Ali, S. Nasir, W. Ensinger, and S. Mafe, Phys. Rev. Appl. **7**, 064035 (2017).

[15]P. Ramirez, J. Cervera, V. Gomez, M. Ali, S. Nasir, W. Ensinger, and S. Mafe, J. Membr. Sci. **573**, 579 (2019).

[16]Y. V. Pershin and M. D. Ventra, Adv. Phys. **60**, 145 (2011).

[17]S. Nasir, M. Ali, J. Cervera, V. Gomez, M. H. A. Haider, W. Ensinger, S. Mafe, and P. Ramirez, J. Colloid Interface Sci. **553**, 639 (2019).

[18]M. Ali, P. Ramirez, H. Q. Nguyen, S. Nasir, J. Cervera, S. Mafe, and W. Ensinger, ACS Nano **6**, 3631 (2012).

[19]R. Epsztein, E. Shaulsky, N. Dizge, D. M. Warsinger, and M. Elimelech, Environ. Sci. Technol. **52**, 4108 (2018).

[20]L. Cao, W. Guo, Y. Wang, and L. Jiang, Langmuir **28**, 2194 (2012).

[21]Y. A. Perez Sirkin, I. Szleifer, and M. Tagliazucchi, Macromolecules **53**, 2616 (2020).

[22]N. Kavokine, R. R. Netz, and L. Bocquet, Annu. Rev. Fluid Mech. **53**, 377 (2021).

[23]J. S. Najem, G. J. Taylor, R. J. Weiss, M. S. Hasan, G. Rose, C. D. Schuman, A. Belianinov, C. P. Collier, and S. A. Sarles, ACS Nano **12**, 4702 (2018).